Soil Dynamics and Earthquake Engineering 162 (2022) 107501

Contents lists available at ScienceDirect

Soil Dynamics and Earthquake Engineering

journal homepage: www.elsevier.com/locate/soildyn

Gaussian random field based correlation model of building seismic performance for regional loss assessment

Tian You [a,b], Wei Wang [a,b,*], Yiyi Chen [a,b], Solomon Tesfamariam [c]

[a] State Key Laboratory of Disaster Reduction in Civil Engineering, Tongji University, Shanghai, 200092, China
[b] Deptartment of Structural Engineering, Tongji University, Shanghai, 200092, China
[c] School of Engineering, The University of British Columbia, Kelowna, B.C., V1V 1V7, Canada

ARTICLE INFO

Keywords:
Structural correlation
Building portfolio
Regional seismic loss assessment
Gaussian random field

ABSTRACT

In order to model the spatial correlations of seismic performances within a portfolio of buildings, an approach based on multiple-output Gaussian random field is proposed in this paper. Seismic performances, including engineering demand parameters, economic loss, repair time, and collapse state, are modeled as functions of latent Gaussian random fields. The correlations of seismic performances are specified by the kernel functions of Gaussian random fields, whose hyperparameters are determined by using Gaussian process regression. After applying the proposed method to a spatially distributed building portfolio, it is demonstrated that overlooking spatial correlations may lead to an underestimate of the probability of occurrence of extreme seismic losses.

1. Introduction

In probabilistic regional loss assessment, for a scenario earthquake and portfolio of buildings, Monte-Carlo simulations of seismic performances are commonly undertaken [1–3]. Seismic performance assessment includes quantifying engineering demand parameter (EDP), economic loss, repair time, and collapse state. The simulations of regional losses are used to generate empirical cumulative distribution function (CDF) from which the exceedance probability of a certain loss can be derived. A straight-forward and accurate way of obtaining a single regional loss simulation is to perform a physics-based ground motion simulation of a scenario earthquake [4–6], and then the simulated ground motion histories are used to perform nonlinear time–history analyses (NTHAs) for individual buildings [7]. Powerful supercomputers are required for such a single large-scale simulation of scenario earthquake and NTHAs, which means that it is not practical to implement a large number of Monte-Carlo simulations.

An alternative state-of-the-art method of performing city-scale regional seismic loss assessment is to simulate an intensity measure (IM) field [8–13] instead of ground motion histories. IMs can be peak ground acceleration (PGA), 5%-damped spectral acceleration (S_a), or advanced IM (e.g. vector-based and average spectral acceleration) [1,14,15]. After IM field simulations, the seismic losses of individual buildings are randomly generated conditioned on the simulated IMs at the building sites. The conditional probability distributions of building seismic losses can be obtained by performing probabilistic seismic performance assessment (PSPA) of individual buildings. PSPA can be done per performance-based seismic design paradigm [16,17] such as the methodology introduced in FEMA P-58 [18]. An advantage of such an approach, in which regional losses are simulated based on IM simulation, is that the scenario analysis is not computationally intensive, because PSPA of individual buildings can be decoupled and the results of PSPA serve as input of scenario analysis.

For the IM-simulation-based regional loss assessment, the realizations of seismic losses of individual buildings should not be generated independently, because the seismic performances of two similar buildings are correlated with each other. The correlations (which is also named dependence in the papers about nuclear plants [19–22]) of seismic performance result from similarities in both ground motion history and structural characteristics. The similarity in ground motion is partially reflected in spatial correlations of IM [8,9,11,12]. However, even if the correlations of IM have been considered, the correlation of building seismic performance has yet to be studied. The following example is presented to demonstrate the effects of spatial distance between buildings. Suppose that there are 10 identical buildings with exactly the same structural parameters (e.g. number of stories, plan area, structural type, beam and column sizes, and material strength). It is already quantified that the collapse probability of each building conditioned on $S_a = 1$ g is equal to 10%. The question is to estimate the probability that all 10 buildings collapse simultaneously when S_a they experience during a scenario earthquake are all equal to 1 g. The answer to this question depends on the spatial distances between these

* Corresponding author at: Deptartment of Structural Engineering, Tongji University, Shanghai, 200092, China.
E-mail address: weiwang@tongji.edu.cn (W. Wang).

https://doi.org/10.1016/j.soildyn.2022.107501
Received 22 March 2022; Received in revised form 13 July 2022; Accepted 7 August 2022
Available online 18 August 2022

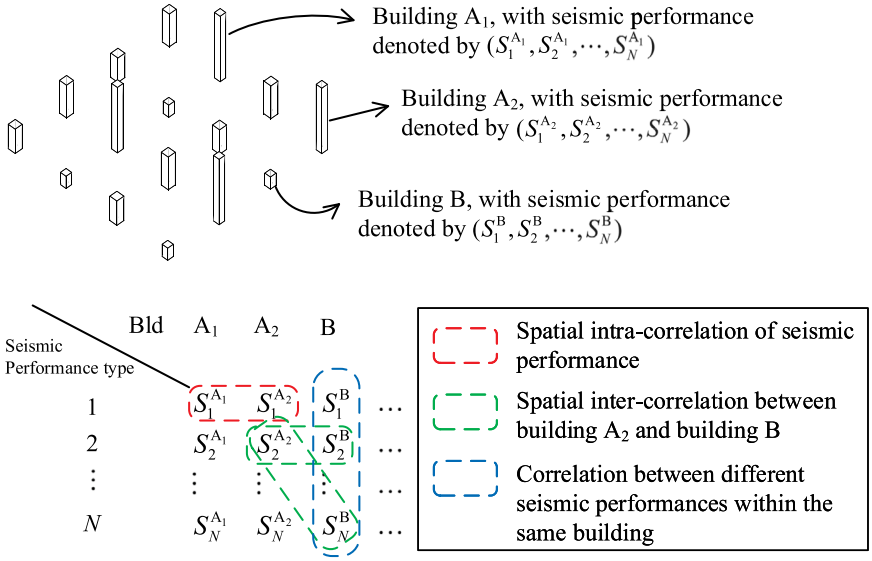

Fig. 1. Schematics of building seismic performances and different types of correlations.

buildings. If these buildings are closely distributed, the ground motions at the sites should be almost identical. So, these buildings will have the same collapse or non-collapse states. In other words, their seismic performances are strongly correlated. In this case, the probability that all 10 buildings simultaneously collapse is close to $P_{\text{upper}} = 10\%$. On the other hand, if buildings are very sparsely distributed, which means their collapse states have much weaker correlations, then the probability of simultaneously collapsing P_{lower} should be much smaller than 10%. In the extreme case of complete independence, the probability P_{lower} is close to $0.1^{10} = 10^{-8}\%$. For a portfolio of buildings in which the spatial distance is neither zero nor infinity, the probability of simultaneously collapsing should lie somewhere in the middle, between P_{lower} and P_{upper}. This example demonstrates that the probability of occurrence of extreme seismic loss will be underestimated if the correlation of seismic performance is omitted (i.e. assuming independence).

Most previous research about regional loss assessment only considers IM correlations [1,2,23,24] and assumes that seismic performances conditioned on a known IM are independent between different buildings. This may underestimate the probability of occurrence of extreme regional loss. So far, very little attention has been paid to the correlation of seismic performances. DeBock et al. [25],DeBock and Liel [26] proposed a method that transmits the correlation of IM to building responses, but state-of-the-art performance-based seismic design approach in FEMA P-58 cannot fit into their framework. Heresi and Miranda [27] proposed a correlation model to consider the correlation of binary seismic outcome (damage or non-damage state) of buildings, but as they mentioned in their paper they did not provide a method to calibrate the model for general implementation.

In this paper, a Gaussian random field (GRF) based model is proposed to consider the spatial correlation of seismic performances between different buildings. Different types of seismic performance metrics, such as EDP, economic loss, repair time, collapse state, can be contained in the model. The probabilistic distributions of seismic performances of individual buildings are obtained from PSPA paradigm like FEMA P-58. In the proposed model, seismic performances are modeled as functions of latent GRFs. The hyperparameters of GRFs are determined using Gaussian process regression [28]. This model provides a new method of utilizing history earthquake data to estimate spatial correlations.

The remaining sections of this paper first introduce some basic concepts and symbols about seismic performance of individual buildings. Then, a GRF-based correlation model of seismic performance is proposed and how to determine the hyperparameters is discussed. Afterwards, the GRF-based approach is applied to a portfolio of buildings. The impact of considering correlations on probabilistic regional loss assessment is investigated based on the case-study results.

2. Seismic performance of individual buildings

There are buildings with different structural characteristics within a building portfolio. As shown in Fig. 1, buildings A_1 and A_2 are located at two different sites, but they have exactly the same structural parameters. Building B is another type of building. Their seismic performances are denoted by $(S_1^{A_1}, S_2^{A_1}, \ldots, S_N^{A_1})$, $(S_1^{A_2}, S_2^{A_2}, \ldots, S_N^{A_2})$, and $(S_1^{B}, S_2^{B}, \ldots, S_N^{B})$, respectively. N is the number of types of seismic performance metrics. For instance, S_1 can be the maximum interstory drift ratio (IDR) during an earthquake. S_2 can be the collapse state of building. $S_2 = 1$ indicates collapse while $S_2 = 0$ indicates non-collapse. S_3 can be the economic loss.

These seismic performances S are random variables. In different realizations of earthquakes, they can be different values. The CDF of seismic performance S of a single building conditioned on a certain intensity IM is denoted by $F_S(s|IM)$. $F_S(s|IM)$ can be obtained according to PSPA, in which a set of ground motion records are scaled to match IM and NTHAs are performed for these scaled records. Buildings A_1 and A_2 have the same CDF of seismic performance, i.e. $F_{S_1^{A_1}}(s|IM) = F_{S_1^{A_2}}(s|IM)$. However, random variables $S_1^{A_1}$ and $S_1^{A_2}$ are not independent in a scenario earthquake even when the IMs for these two buildings are the same. When the spatial distance h between buildings A_1 and A_2 approaches 0, buildings A_1 and A_2 would experience the same ground motion and seismic response, so $S_1^{A_1}$ and $S_1^{A_2}$ are perfectly correlated (i.e. exactly the same). On the other hand, if the spatial distance h is greater, the correlation between $S_1^{A_1}$ and $S_1^{A_2}$ would decrease.

Considering the spatial correlation of seismic performances between different buildings is the focus of this paper. When two buildings (like buildings A_1 and A_2) have exactly the same structural parameters, the spatial correlation of the same type of seismic performance S_i is named spatial intra-correlation, as shown by the red dashed box in Fig. 1. The spatial correlation between two different buildings (like buildings A_2 and B) is named spatial inter-correlation, as shown by the green dashed boxes in Fig. 1. Note that the seismic performances within the same building, e.g. S_i^B and S_j^B, are also correlated. But this correlation is beyond the scope of this paper because it can be obtained by only performing PSPA of a single building [16–18] without a scenario analysis.

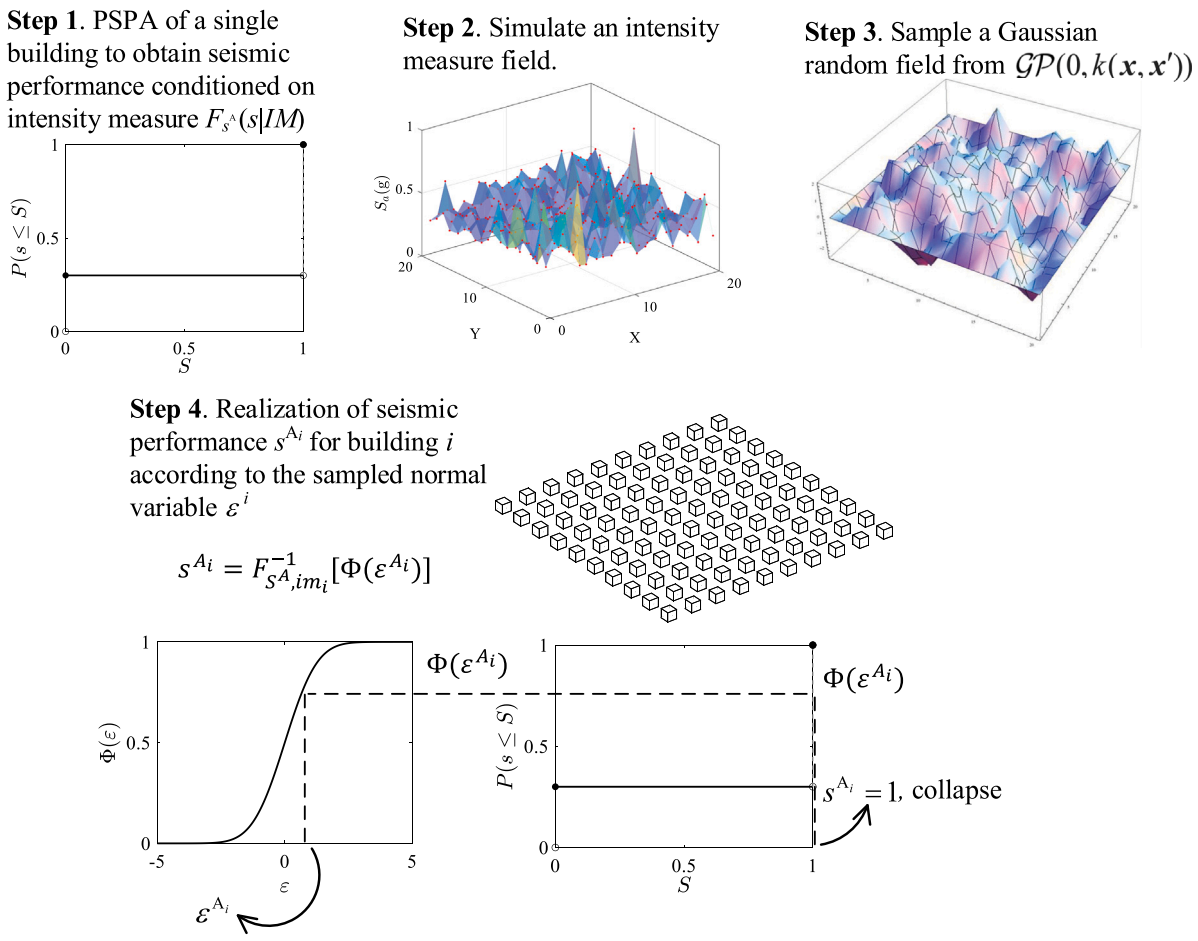

Fig. 2. Procedure of simulating regional seismic loss based on Gaussian random field.

3. Correlation model of seismic performance

3.1. Introduction to Gaussian random field

Before presenting the GRF-based correlation model, a brief introduction to GRF is given here. A GRF is a Gaussian process whose input, $\boldsymbol{x} = (x_1, x_2)$, is two-dimensional and whose output $\varepsilon(\boldsymbol{x})$ is a scalar [28]. Every finite collection of output random variables $\boldsymbol{\varepsilon}$ have a multivariate normal distribution. A particular stationary, isotropic GRF is applied in this paper. Stationarity means mean and variance of the GRF do not change over input space. Isotropy means the correlation of outputs at two locations, $\varepsilon(\boldsymbol{x})$ and $\varepsilon(\boldsymbol{x}')$, depends only on $|\boldsymbol{x} - \boldsymbol{x}'|$, the Euclidean distance between $\boldsymbol{x}$ and $\boldsymbol{x}'$. This GRF is denoted by $\varepsilon(\boldsymbol{x}) \sim \mathcal{GP}(0, k(\boldsymbol{x}, \boldsymbol{x}'))$, where 0 means a zero mean and $k(\boldsymbol{x}, \boldsymbol{x}')$ denotes the kernel function. The kernel function defines the correlation of outputs at two locations [28,29]:

$$k(\boldsymbol{x}, \boldsymbol{x}') = E[\varepsilon(\boldsymbol{x}) \cdot \varepsilon(\boldsymbol{x}')], \tag{1}$$

where $E(\cdot)$ denotes the expectation of a random variable. Such a GRF is completely specified by the kernel function. Note that $k(\boldsymbol{x}, \boldsymbol{x}')$ equals the covariance between $\varepsilon(\boldsymbol{x})$ and $\varepsilon(\boldsymbol{x}')$ because $E[\varepsilon(\boldsymbol{x})] = E[\varepsilon(\boldsymbol{x}')] = 0$. $k(\boldsymbol{x}, \boldsymbol{x}')$ also equals the correlation coefficient only if the variances of $\varepsilon(\boldsymbol{x})$ and $\varepsilon(\boldsymbol{x}')$ are equal to 1. As the GRF is isotropic, the kernel function can be written as a function of spatial distance $h = |\boldsymbol{x} - \boldsymbol{x}'|$, i.e. $k(\boldsymbol{x}, \boldsymbol{x}') = k(h)$.

A kernel function has to satisfy some constraints in order to ensure that the covariance matrix of every finite collection of output $\boldsymbol{\varepsilon}$ is positive semi-definite (PSD) [28]. Common kernel functions that satisfy PSD condition include exponential function $k(h) = e^{-h/l}$ and squared exponential function $k(h) = e^{-h^2/(2l^2)}$, where l is a hyperparameter that defines the decay rate of correlation. A smaller l indicates a higher decay rate.

3.2. Intra-correlation of seismic performance

The intra-correlation of a seismic performance S^A is the spatial correlation between buildings that have exactly the same structural parameters but are located at different sites. Suppose that there is a portfolio of buildings that are located at different sites. The procedure of simulating a regional seismic loss in which intra-correlation is considered is as follows, as shown in Fig. 2.

(a) Perform PSPA of a single building in order to obtain the CDF of the seismic performance conditioned on any given intensities $F_{S^A}(s|IM)$. The subfigure in step 1 of Fig. 2 gives an example of the CDF of collapse state conditioned on a certain IM. The probability of collapse (denoted by $S = 1$) is equal to 0.7 and probability of non-collapse (denoted by $S = 0$) is equal to 0.3. As the collapse state conditioned on a certain intensity $S|$IM is either 1 or 0, the CDF is a step function.

(b) Simulate a spatially correlated IM field. The median logarithm of IM can be estimated using ground motion prediction equation [30,31]. Empirical models can be applied to consider the spatial correlation of within-event (intra-event) residual [2,10,12,13,32]. Then, the simulated seismic intensity im_i corresponding to the ith building can be obtained from the IM field.

(c) Sample a GRF from $\mathcal{GP}(0, k(\boldsymbol{x}, \boldsymbol{x}'))$. According to the sampled field of $\varepsilon^A(\boldsymbol{x})$, each building corresponds to a ε^{A_i} at the building

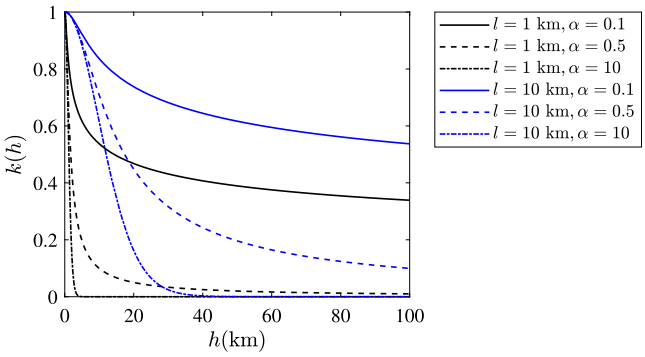

Fig. 3. Example rational quadratic kernel functions.

site. How to determine the hyperparameters of kernel function will be discussed in Section 3.4.

(d) Realization of seismic performance s^{A_i} for each building. The seismic performance s^{A_i} is calculated as follows:

$$s^{A_i} = F^{-1}_{S^A, im_i}[\Phi(\varepsilon^{A_i})], \tag{2}$$

where i represents the ith building; $\Phi(\cdot)$ denotes the CDF of standard normal distribution; and $F^{-1}_{S^A, im_i}(\cdot)$ denotes the inverse function of $F_{S^A}(s|im_i)$ in which im_i denotes the simulated seismic intensity at the building site. The interpretation of Eq. (2) is shown at the bottom of Fig. 2. When the generated ε^{A_i} lies between $\Phi^{-1}(0.3)$ and $+\infty$, $\Phi(\varepsilon^{A_i})$ would lie between 0.3 and 1, and the simulated collapse state s^{A_i} would be equal to 1 which means the ith building collapses in this simulation. In Eq. (2), the seismic performances are modeled as a function of a latent GRF ε. The reason ε is called latent is because for an observed seismic performance s, there may be numerous possible ε that maps to s. In the case shown in Fig. 2, ε^{A_i} that lies between $\Phi^{-1}(0.3)$ and $+\infty$ can all map to a collapse state (in which $s^{A_i} = 1$). Only when the CDF of seismic loss $F_{S^A}(s|IM)$ is a strictly increasing function, there is a one-to-one mapping from ε^{A_i} to s^{A_i}. The CDFs of economic loss and repair time may be strictly increasing, but the CDFs of collapse state or the number of casualties are not.

Such a procedure of simulating regional seismic loss can ensure that (1) the probability distribution of seismic losses of a single building is in accordance with $F_{S^A}(s|IM)$ obtained in step 1; and (2) there is a correlation between S^{A_i} and S^{A_j} which represent the seismic performances of buildings located at two different sites. When the spatial distance h approaches 0, ε^{A_i} will approach ε^{A_j}, and S^{A_i} will approach S^{A_j}, which means S^{A_i} and S^{A_j} become equal. When the spatial distance h becomes greater, the correlation between S^{A_i} and S^{A_j} decreases. The hyperparameters of kernel function $k(\boldsymbol{x}, \boldsymbol{x}')$ controls the decay rate of correlation, and they can be fitted to real scenario earthquake responses which were observed in the history. It should be noted that the Pearson's correlation coefficient between S^{A_i} and S^{A_j} is not exactly equal to the one between ε^{A_i} and ε^{A_j}. They are equal only when S^{A_i} follows a normal distribution [27].

The procedure above is the same as the one proposed by Heresi and Miranda [27] except how the covariance matrix K of variable ε is derived. In their research [27], they assumed ρ_{ij} (that is an element of K) to be an explicit function of separation distance and year of construction $\rho_{ij} = f(\Delta_{ij}, \mathrm{d}T_{ij})$. The problem of this model is that the obtained covariance matrix K is not guaranteed to be PSD. In the intra-correlation model of our study, it is assumed that there is a latent GRF $\varepsilon(\boldsymbol{x})$, and the covariance matrix K is derived from the kernel function of GRF $k(\boldsymbol{x}, \boldsymbol{x}')$. The advantages of this model include: (1) it guarantees the obtained covariance matrix K to be PSD regardless of the values of hyperparameters; (2) it provides a theoretical basis that enables the use of maximum likelihood estimation to calibrate the model. In this way, the intra-correlation of a single building is represented by a GRF. More importantly, the inter-correlation between different buildings (that have different structural characteristics) is modeled as the inter-correlation between different GRFs, which will be presented in the following section. Another difference is the selection of IM. PGA was selected as the IM in the research [27], while the 5%-damped spectral acceleration at the fundamental period of each building is selected as the IM in our study.

3.3. Inter-correlation of seismic performance

As for the inter-correlation of seismic performances of two different buildings, e.g. S^A and S^B, a GRF with a scalar output is not sufficient. S^A corresponds to a latent GRF ε^A, while S^B corresponds to another latent GRF ε^B. The inter-correlation between S^A and S^B is reflected in the inter-correlation between two GRFs ε^A and ε^B. For a more general situation, there are D types of buildings, then a GRF with D-dimensional output is denoted by $\{\varepsilon^d(\boldsymbol{x})|d = 1, \ldots, D\}$. Each dimension of output corresponds to a unique type of building. The difficulty of configuring a multiple-output GRF is that the covariance matrix has to be positive semi-definite.

The semiparametric latent factor model (SLFM) [33] is applied in this paper to configure a multiple-output GRF. SLFM assumes that the D-dimensional output can be written as a linear combination of a series of independent scalar-output GRF:

$$\varepsilon^d(\boldsymbol{x}) = \sum_{q=1}^{Q} A_{dq} u_q(\boldsymbol{x}), \tag{3}$$

where A_{dq} are parameters and form a matrix denoted by $\mathbf{A}$, and $u_q(\boldsymbol{x})$ are a series of independent scalar-output GRF. The kernel function of $u_q(\boldsymbol{x})$ is denoted by $k_q(\boldsymbol{x}, \boldsymbol{x}')$. In this inter-correlation model, hyperparameters include the elements of matrix $\mathbf{A}$ and the parameters in $k_q(\boldsymbol{x}, \boldsymbol{x}')$. Given these hyperparameters, the covariance of $\varepsilon^d(\boldsymbol{x})$ can be calculated as follows:

$$\begin{aligned}\mathrm{cov}[\boldsymbol{\varepsilon}(\boldsymbol{x}), \boldsymbol{\varepsilon}(\boldsymbol{x}')] &= \begin{bmatrix} \mathrm{cov}[\varepsilon^1(\boldsymbol{x}), \varepsilon^1(\boldsymbol{x}')] & \cdots & \mathrm{cov}[\varepsilon^1(\boldsymbol{x}), \varepsilon^D(\boldsymbol{x}')] \\ \vdots & \ddots & \vdots \\ \mathrm{cov}[\varepsilon^D(\boldsymbol{x}), \varepsilon^1(\boldsymbol{x}')] & \cdots & \mathrm{cov}[\varepsilon^D(\boldsymbol{x}), \varepsilon^D(\boldsymbol{x}')] \end{bmatrix} \\ &= \sum_{q=1}^{Q} \boldsymbol{a}_q \boldsymbol{a}_q^T k_q(\boldsymbol{x}, \boldsymbol{x}') = \sum_{q=1}^{Q} B_q k_q(\boldsymbol{x}, \boldsymbol{x}')\end{aligned} \tag{4}$$

where $\boldsymbol{a}_q$ is the qth column of $\mathbf{A}$, and $B_q = \boldsymbol{a}_q \boldsymbol{a}_q^T$.

The procedure of simulating regional seismic loss in which inter-correlation exists is similar to the procedure shown in Fig. 2. The only differences are that (1) in step 2, multiple IM fields (corresponding to different fundamental periods of buildings) should be generated and the cross-correlations between different IM fields should be considered [8,9,11]; and (2) in step 3, $\varepsilon^d(\boldsymbol{x})$ are generated according to the covariance provided in Eq. (4).

3.4. Gaussian process regression for determining hyperparameters

The spatial correlations of seismic performance are specified by kernel functions. Many different forms of kernel functions are available. A k-fold cross-validation method can be used to select the best kernel function after defining a loss function [28]. The k-fold cross-validation means that the data (from the Northridge earthquake) is split into k disjoint, equally sized subsets; validation is done on a single subset and regression is done using the union of the remaining $k - 1$ subsets. The entire procedure is repeated k times and each time a different subset is used for validation. After using this method to compare several common forms of kernel functions, the rational quadratic kernel function is selected as the one used in this study, as a trade-off between fitting

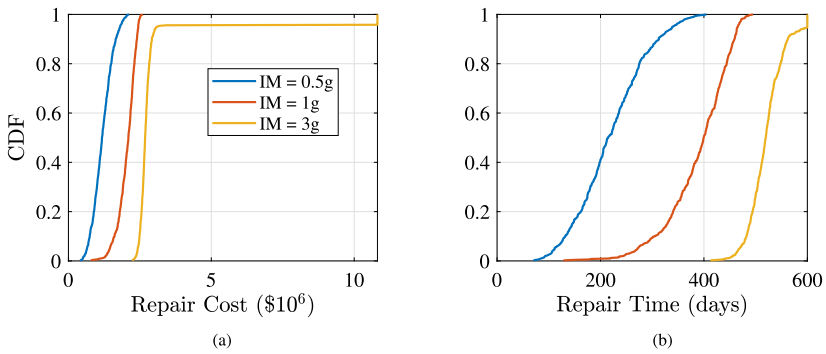

Fig. 4. CDFs of (a) repair cost and (b) repair time of a three-story MRF per level of seismic intensity.

accuracy and the number of hyperparameters. The rational quadratic kernel function [29] is defined by:

$$k(h) = \sigma_f^2 \left(1 + \frac{h^2}{2\alpha l^2}\right)^{-\alpha}. \tag{5}$$

There are three parameters including σ_f^2, l, and α. σ_f^2 is always equal to 1 in our models, because ε we utilize follows a standard normal distribution with a standard deviation of 1. l and α control the shape of the curves. This rational quadratic function can actually represent various types of decay rate of correlation as shown in Fig. 3.

The hyperparameters of kernel functions should be calibrated using real scenario earthquake observations. Suppose that a set of seismic performances $\boldsymbol{s}^*$ were observed within a scenario earthquake. Each element in vector $\boldsymbol{s}^*$ represents an observed seismic performance of a single building. The number of observed buildings is n. The vector of observed latent variables $\boldsymbol{\varepsilon}$ of these buildings is denoted by $\boldsymbol{\varepsilon}^*$, which is derived from $\boldsymbol{s}^*$ according to Eq. (2). As $\boldsymbol{\varepsilon}$ is n-variate normally distributed, the probability of $\boldsymbol{\varepsilon}^*$ being observed is calculated as follows [28]:

$$\ln p(\boldsymbol{\varepsilon}^*|\boldsymbol{\theta}) = -\frac{1}{2}\boldsymbol{\varepsilon}^{*T} K^{-1}\boldsymbol{\varepsilon}^* - \frac{1}{2}\ln|K| - \frac{n}{2}\ln 2\pi, \tag{6}$$

where $\boldsymbol{\theta}$ denotes the vector of hyperparameters, and K denotes the prior covariance matrix of $\boldsymbol{\varepsilon}$. Prior covariance K can be calculated per Eq. (1) or (4). A Gaussian process regression [28] is a kind of maximum likelihood estimation that maximizes the likelihood function in Eq. (6) by finding the optimal value of hyperparameters $\boldsymbol{\theta}$.

If a one-to-one mapping from the observed seismic performances $\boldsymbol{s}^*$ to the latent variables $\boldsymbol{\varepsilon}^*$ does not exist, Eq. (6) then cannot be directly applied. However, the observed latent variables $\boldsymbol{\varepsilon}^*$ should lie in certain intervals. For example, the observed collapse state in Fig. 2 is $s^* = 1$, and the observed latent variable ε^* lies in the interval $(\Phi^{-1}(0.3), +\infty)$. In this case, the following likelihood function can be applied:

$$p = \int_{a_1}^{b_1} \cdots \int_{a_n}^{b_n} \phi(\boldsymbol{\varepsilon}|\boldsymbol{\theta})\, d\varepsilon_1 \cdots d\varepsilon_n, \tag{7}$$

where $[a_i, b_i]$ denotes the observed interval of latent variable ε_i^*, and $\phi(\boldsymbol{\varepsilon}|\boldsymbol{\theta})$ denotes the probability density function of multivariate normal distribution given hyperparameters $\boldsymbol{\theta}$.

4. Case study of regional loss assessment

4.1. Building models and probabilistic seismic performance assessment

To conduct a case study of regional loss assessment, 4 types of steel structures [34] are selected here to constitute a portfolio of buildings. The 4 typical steel structures include a three-story moment-resisting frame (MRF), a nine-story MRF, a three-story self-centering buckling-restrained braced frame (SC-BRBF), and a nine-story SC-BRBF. These 4 buildings are denoted by building A, B, C, and D, respectively. The PSPA of these buildings is performed to obtain the CDFs of seismic performances $F_S(s|IM)$. These seismic performances include EDPs (e.g. maximum IDR, peak floor acceleration, peak floor velocities, and residual drifts), collapse state, economical loss, and repair time.

These structures are modeled as 2D finite element models using the nonlinear dynamic analysis program OpenSees [35]. Beams and columns are modeled with displacement-based beam–column element, and braces are modeled with self-centering material. Lean columns are utilized to consider the P-Δ effect. The 22 pairs of far-field ground motion records in FEMA P-695 [36] are scaled to match a series of spectral accelerations ranging from 0.1 to 5 g, and NTHAs are performed to obtain the EDPs under these intensities. In order to calculate the probability distributions of repair cost and repair time, Normative Quantity Estimation Tool [18] is applied to estimate the quantity of nonstructural components. Probabilistic assessment of repair cost and repair time is conducted using the PACT tool introduced in FEMA P-58 [18]. To illustrate the results of PSPA of individual buildings, the CDFs of repair cost and repair time of the three-story MRF are plotted in Fig. 4 per level of seismic intensity. The yellow CDFs (IM = 3 g) have a sudden rise at the end of the curves because the collapse probability of the building is about 5%.

4.2. Development of correlation model

Before performing a regional seismic loss assessment per the proposed procedure in Section 3.2, the hyperparameters in the correlation model must be determined. As discussed in Section 3.4, Gaussian process regression is applied to fit the rational quadratic kernel functions to come to a maximum likelihood of the observed seismic performances. The observed seismic performances are obtained using the ground motion acceleration history recorded during the 1994 Northridge earthquake. 136 pairs of ground motion records of the 1994 Northridge earthquake are retrieved from PEER NGA-West2 ground motion database [37]. NTHAs are performed under these ground motions for each of the 4 buildings.

The intra-correlation models of EDPs, repair cost, and repair time are developed for the 4 buildings. For example, the maximum IDRs of the three-story MRF under 136 records can form an observation of IDR, denoted by s^*_{IDR}, which is a 136 × 1 vector. These IDRs are plotted in Fig. 5(a) together with the locations of stations. Then, according to Eq. (2), the corresponding $\boldsymbol{\varepsilon}^*$ variables can be calculated and they are shown in Fig. 5(b). In Fig. 5(b), only 69 out of 136 elements of $\boldsymbol{\varepsilon}^*$ are retained because those ground motion records whose intensities S_a are smaller than 0.1 g are discarded. By maximizing the likelihood function in Eq. (6), the optimal hyperparameters $\boldsymbol{\theta}$ (i.e. parameters of the rational quadratic kernel function) can be found. The *fmincon* function in Matlab is utilized as the algorithm for finding the optimal hyperparameters. The covariance of $\varepsilon^{\mathrm{A}}_{\mathrm{IDR}}(\boldsymbol{x})$, which is the latent ε variable corresponding to the maximum IDR of the three-story building (denoted by building A), is plotted in Fig. 6(a) as a function of spatial distance between two buildings. Similarly, the intra-correlation models of repair time and repair cost can also be obtained. The covariance function $\mathrm{cov}(\varepsilon^{\mathrm{A}_i}_{\mathrm{RC}}, \varepsilon^{\mathrm{A}_j}_{\mathrm{RC}})$ of repair cost is shown in Fig. 6(b).

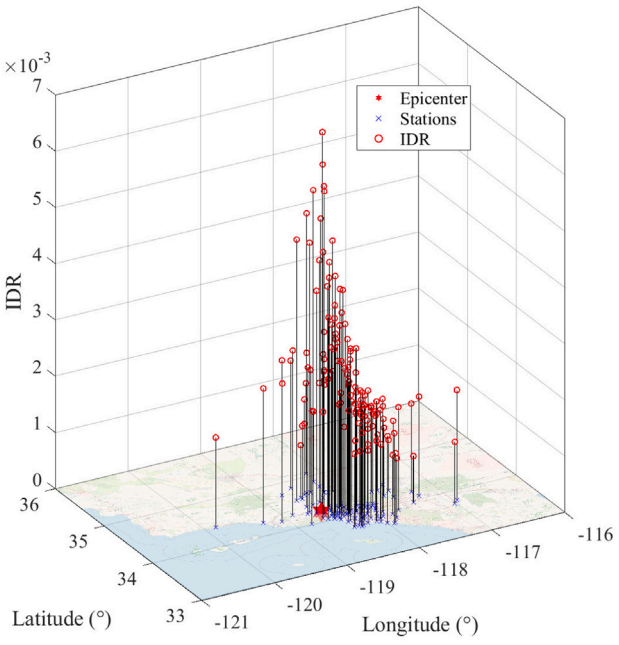

(a)

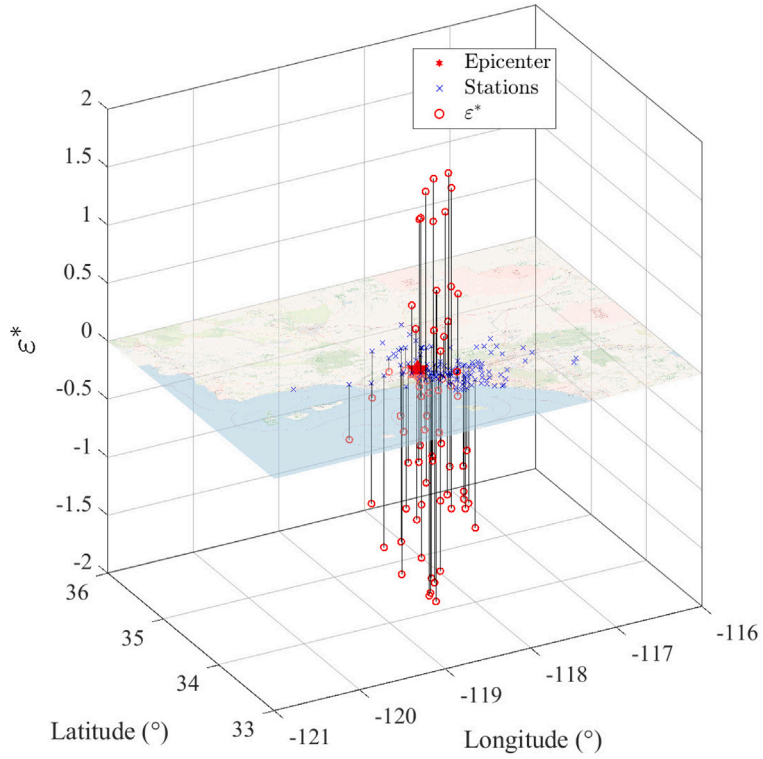

(b)

Fig. 5. Scenario analysis of Northridge earthquake: (a) the maximum interstory drift ratios of a three-story MRF and (b) the corresponding ϵ^* variables.

Apart from the covariance functions derived from the GRF-based model, empirical discrete covariance is also plotted in Fig. 6. It can be seen that the covariance from GRF-based models and empirical are consistent. The empirical discrete covariance $\mathrm{cov}_e(h_i)$ for a certain spatial distance h_i is estimated as [38]:

$$\mathrm{cov}_e(h_i) = \frac{1}{N_{e,i}} \sum_{k=1}^{N_{e,i}} \varepsilon^*_{k,1} \varepsilon^*_{k,2}, \tag{8}$$

where $(\varepsilon^*_{k,1}, \varepsilon^*_{k,2})$ is a pair of observed latent ε variables whose spatial distance is approximately equal to h_i. For distance $h_i = 0$, there are 69 pairs of observations (i.e. $N_{e,i} = 69$), because there are 69 valid stations in Fig. 5(b) and each station and itself form a single pair of data. For other discrete distances, there are $\binom{69}{2} = 2346$ pairs of observations in total. They should be separated into different groups according to the distances. Each group has a certain number of pairs of variables

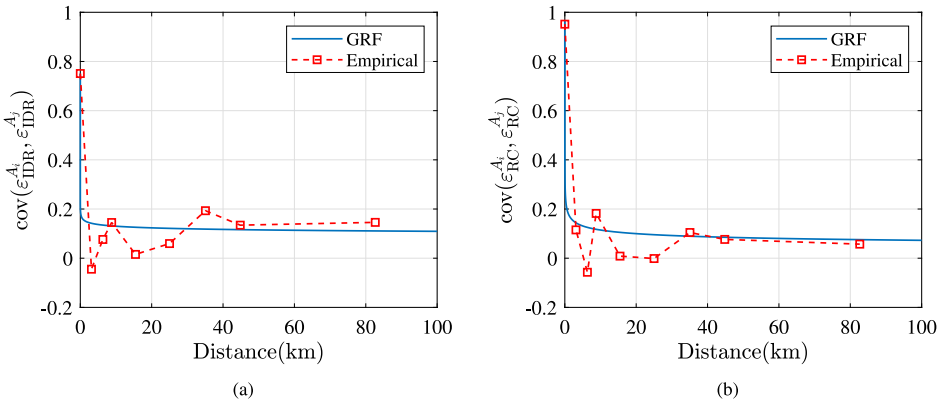

Fig. 6. Covariance functions, $\mathrm{cov}(\varepsilon^{A_i}_{IDR}, \varepsilon^{A_j}_{IDR})$ and $\mathrm{cov}(\varepsilon^{A_i}_{RC}, \varepsilon^{A_j}_{RC})$, obtained from the intra-correlation models of (a) the maximum IDR and (b) the repair cost of a three-story MRF (denoted by building A). ε^{A}_{IDR} and ε^{A}_{RC} denote the latent ε variables corresponding to the maximum IDR and the repair cost respectively. The blue solid curves represent the covariance derived from the GRF-based model and the red dashed curves represent the discrete covariance functions.

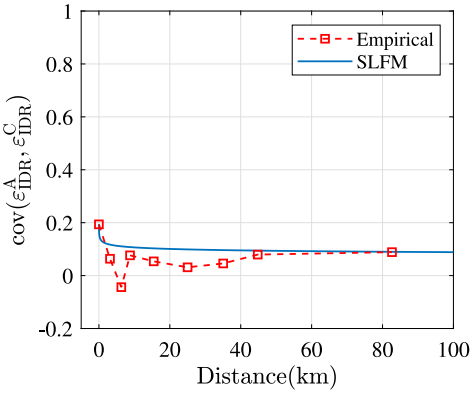

Fig. 7. Covariance functions $\mathrm{cov}(\varepsilon^{A}_{IDR}, \varepsilon^{C}_{IDR})$ obtained from the inter-correlation models. ε^{A}_{IDR} and ε^{C}_{IDR} denote the latent ε variables corresponding to the maximum IDRs of a three-story MRF (denoted by building A) and a three-story SC-BRBF (denoted by building C) respectively. The blue solid curves represent the covariance derived from the SLFM and the red dashed curves represent the discrete covariance functions.

$(\varepsilon^{*}_{k,1}, \varepsilon^{*}_{k,2})$ and these data are used to calculate an empirical covariance per Eq. (8). The number of groups should not be too many or too small. If the number of groups is too many, the quantity of data for each discrete distance is too small to come to a reliable estimate of covariance $\mathrm{cov}_e(h_i)$. On the other hand, if the group number is too small, the correlation of the specific distance cannot be well represented. In Fig. 5(b), the 2346 pairs of ε^{*} variables are grouped into intervals of $(0,5)$, $(5,7.5)$, $(7.5,10)$, $(10,20)$, $(20,30)$, $(30,40)$, $(40,50)$, $(50,+\infty)$ to represent 8 discrete distances. The average distance within each group is calculated to be the representative distance of the group. Together with the $h_i = 0$ distance, there are 9 empirical data points in Fig. 6. It should be noted that using pairs of $(\varepsilon^{*}_{k,1}, \varepsilon^{*}_{k,2})$ that are from the same event is not theoretically correct, but the empirical covariance provides a straightforward verification of the GRF-based correlation model.

The inter-correlation models of EDPs, repair cost, and repair time between the 4 buildings are also developed. As an example, Fig. 7 shows the IDR covariance $\mathrm{cov}(\varepsilon^{A}_{IDR}, \varepsilon^{C}_{IDR})$ of the three-story MRF (denoted by building A) and the three-story SC-BRBF (denoted by building C). Compare with the intra-correlation shown in Fig. 6(a), the inter-correlation between different buildings is much weaker. This complies with our engineering experience that structures with similar characteristics should have similar seismic responses.

The overall correlation models of IDRs and repair cost of the 4 buildings are summarized in Fig. 8. The diagonal subfigures represent the intra-correlation models, and the off-diagonal subfigures represent the inter-correlation models of two different buildings. Note that the correlation patterns of IDRs and repair cost are quite similar, which implies that the correlation models for different types of seismic performance metrics can be seen as the same from a practical perspective. In Fig. 8, the correlations related to building D or B (e.g. D–D, B–B, A–D) are relatively strong compared to others. These correlations are not estimated accurately, because the quantity of usable ground motion records in Northridge earthquake is not sufficient for building B and D. As building B and D have relatively long fundamental periods (2.26 and 1.8 s, respectively), the spectral accelerations of most records in Northridge earthquake are smaller than 0.1 g, which is too small to cause evident seismic losses. Only 22 out of 169 records are usable for building B, and 34 usable for building D.

4.3. Regional seismic loss assessment

In this subsection, the effects of considering correlation of seismic performances on regional loss assessment are investigated. The correlation of seismic performances is a combined effect of both the similarities of ground motion histories and the similarities of structural characteristics. Furthermore, the similarities of structural characteristics can be caused by the similarities of architectural and structural designs (e.g. number of stories and structural types), and the correlations of random structural parameters (e.g. material strength, beam and column sizes) that may be caused by the building contractors. In this section, the 4 different structures are utilized to consider the similarities of architectural and structural designs, but the uncertainties and correlations of structural parameters are omitted. Thus, if two exactly equal buildings have almost 0 separation distance, their seismic responses are considered to be exactly the same. There are two extreme cases that can be seen as upper and lower bounds of regional loss assessment. The first extreme case is to assume independence between seismic losses of different buildings when the spatial distance between buildings is pretty large, which means the latent ε variables of different buildings are generated independently. In the other extreme case where the spatial distance approaches 0, the latent ε variables are almost perfectly correlated. We will provide examples in Sections 4.3.1 and 4.3.2 to argue that it is not always appropriate to assume perfect correlation for closely distributed buildings or assume independence for sparsely distributed buildings.

4.3.1. Closely distributed buildings

In order to investigate whether it is appropriate to assume perfect correlation when the spatial distance is small, a portfolio of buildings that are very closely distributed are hypothesized as shown in Fig. 9. There are $N_b \times N_b$ buildings and the spatial distance of adjacent buildings is equal to d. All these buildings have the same structural parameters as the three-story MRF (i.e. building A) mentioned in

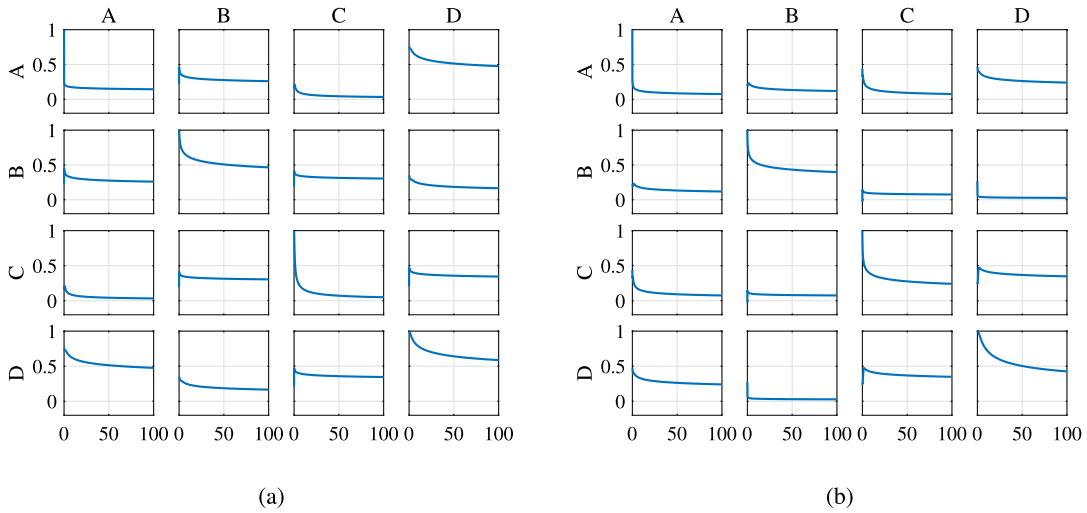

Fig. 8. Covariance functions of latent ϵ variables corresponding to (a) the maximum IDRs and (b) the repair cost of the 4 buildings. A, B, C, and D represent the three-story MRF, the nine-story MRF, the three-story SC-BRBF, and the nine-story SC-BRBF respectively.

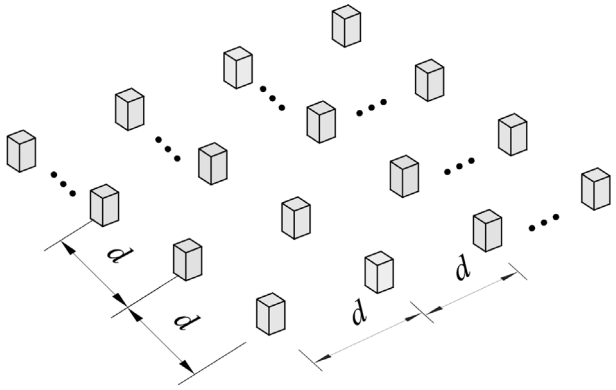

Fig. 9. Distribution of a portfolio of buildings.

Section 4.1. Let $N_b = 10$ and $d = 20$ m. After performing Monte-Carlo simulations according to the procedure introduced in Section 3.2, the CDF of regional repair cost conditioned on a certain intensity $S_a = 1$ g can be obtained. Note that only the intra-correlation model of repair cost of building A is required, and the simulation of IM field in step 2 in Fig. 2 is not necessary because the IM field here is a constant ($S_a = 1$ g). A constant-IM loss assessment of a portfolio of buildings is analogous to an intensity-based loss assessment of a single building for which a design basis earthquake or maximum considered earthquake is considered. The CDFs of regional repair cost when the structural type of all buildings is type A are plotted in Fig. 10(a). It indicates that the regional loss curve of considering partial correlation is much closer to the curve of assuming independence (blue solid curve) rather than the curve of assuming perfect correlation (red solid curve), even though the spatial distance is very small ($d = 20$ m).

The phenomenon that perfect correlation is invalid when spatial distance is very small ($d = 20$ m) can be explained from two aspects. The first aspect is that the intra-correlation of building A has a very high decay rate. As shown in Fig. 6(b), the covariance (also correlation coefficient) is less than 0.3 when $h \geq 80$ m. This weak correlation makes the GRF-based CDF curve closer to the curve assuming independence. To show another CDF curve with slightly stronger intra-correlation than in building A, building A is replaced with building C (a three-story SC-BRBF). The corresponding CDFs of regional repair cost for building C are shown in Fig. 10(b). In Fig. 10(b), the curve considering partial correlation becomes very different from the curve of assuming independence, especially for extreme seismic losses, because building C has a smaller decay rate of intra-correlation than building A. The other aspect is that the regional diameter (the largest distance between buildings) is also an important factor in considering the correlation effects. The correlation effect not only depends on the spatial distance h between two adjacent buildings, but also depends on the largest distance. These two aspects make assuming perfect correlation not an appropriate choice even for a spatial distance of 20 m between adjacent buildings.

In Fig. 10(b), it can be seen that using the GRF-based correlation model leads to a higher probability of occurrence of extreme seismic losses. For example, the probability of seismic losses exceeding $\$170\times10^6$ is 0% when assuming independence, while the probability is 3% when using the GRF-based correlation model.

4.3.2. Sparsely distributed buildings

In order to investigate whether it is appropriate to assume independence when buildings are sparsely distributed, let $N_b = 40$ and $d = 100$ m which means both distance of adjacent buildings and the largest distance are large. All buildings are type A buildings, i.e. three-story MRFs. The CDFs of regional repair cost conditioned on IM = 1 g can be calculated after performing regional loss assessment. As shown in Fig. 11, the curves of considering partial correlation (yellow curve) and assuming independence (blue curve) are distributed in a very narrow range of seismic losses. This narrow range can be explained by the law of large numbers. As the seismic losses of these building are independent, their total losses tend to be close to the expected losses. Though assuming independence (the blue curve in Fig. 11) provides a good estimate of seismic losses for sparsely distributed buildings, the CDF of seismic losses obtained from the GRF-based correlation model (the yellow curve) is still slightly different from that of assuming complete independence.

4.3.3. Regional loss assessment based on IM field simulation

The above regional loss assessment in Sections 4.3.1 and 4.3.2 is conditional on constant IMs. On the other hand, if one wants to perform regional loss assessment conditioned on certain earthquake magnitudes, Monte-Carlo simulations of IM fields are required. The GMPEs presented by Campbell and Bozorgnia [30] are applied in this paper to estimate mean and variance of IM. The spatially cross-correlated within-event residuals are simulated using the principle component analysis (PCA) based method proposed by Markhvida et al. [12], and the cross-correlated between-event residuals are simulated using the empirical models of interevent correlation coefficients [8,9,11].

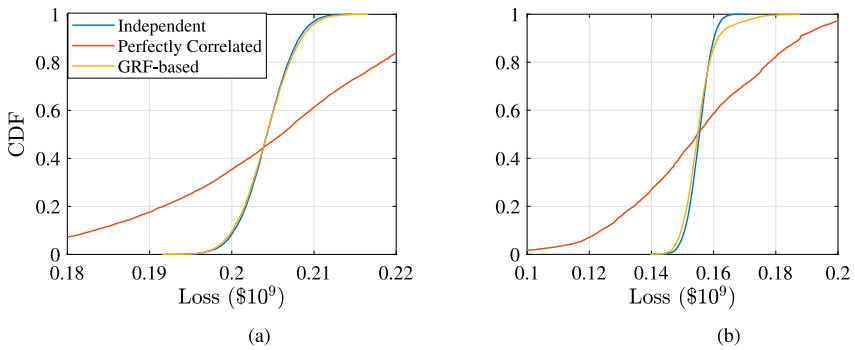

Fig. 10. CDFs of regional repair cost for (a) three-story MRFs and (b) three-story SC-BRBFs when $N_b = 10$, $d = 20$ m, and IM=1 g.

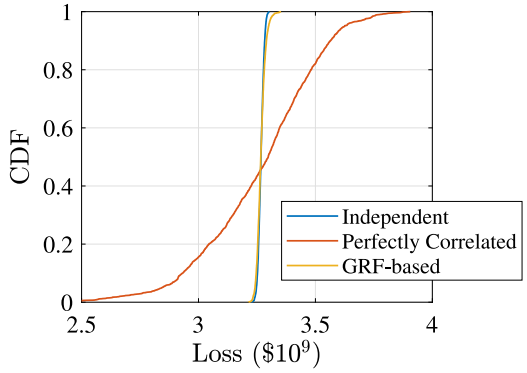

Fig. 11. CDFs of regional repair cost for three-story MRFs conditioned on $S_a = 1$ g when $N_b = 40$ and $d = 100$ m.

Let $N_b = 10$ and $d = 50$ m. 4 types of buildings are alternately distributed. Suppose that the epicenter is located at the center of the portfolio of buildings and a 45°-dipping normal fault is considered. The down-dip width of fault rupture equals 10 km and hypocentral depth equals 15 km. As an example of applying GMPE and simulating an IM field, the median intensity $S_a(T = 1.1\text{ s})$ estimated from GMPEs is shown in Fig. 12(a), and a simulated field of intensity $S_a(T = 1.1\text{ s})$ that considers the uncertainty and correlation of IM is shown in Fig. 12(b). By comparing the two figures, it can be seen that the IM uncertainty is quite evident.

After simulating a large number of IM fields and regional losses of buildings, the CDFs of regional repair cost can be obtained. The solid curves in Fig. 13 represent the CDFs in which the IM uncertainties are considered, i.e. a large number of IM fields like in Fig. 12(b) are generated. All solid curves, including assuming independence, perfect correlation, or partial correlation, are almost the same, which means that the correlation of seismic performance has no impact on magnitude-based regional loss assessment as long as the uncertainties and correlations of IM have been considered. This conclusion can be made clear by investigating the regional loss when IM uncertainties are discarded. The dashed curves in Fig. 13 represent the CDFs of regional losses in which IMs are equal to the median values. When IM uncertainties are not considered, the correlation of seismic performances significantly influence the probability distribution of regional losses.

Although the spatial correlation of seismic performances shows a relatively small influence in the case of considering IM uncertainties, this may not be a general conclusion. The negligible effect of spatial correlation on the distribution of total losses is due to the fast decay rate of spatial correlation of seismic performances, which is, in turn, caused by the fast decay of spatial correlation of ground-motion intensity residuals of the Northridge earthquake [39]. The ground-motion records of the Northridge earthquake are the only data that were used to calibrate the GRF-based model in this study. For other events, the spatial correlation of intensity residuals may be stronger. Therefore, the spatial correlation may have more evident influences on the distribution of total losses, if ground-motion records from other events are used. A more reasonable strategy of calibrating correlation models is to select records from different history events. Then, the obtained correlation models can represent an average level of decay rate of spatial correlation.

5. Summary and conclusions

This paper proposes a GRF-based method to model the spatial correlations of seismic performances within a portfolio of buildings. Different types of seismic performance metrics, including EDPs, economic loss, repair time, etc., are modeled as the functions of latent GRFs $\varepsilon(\boldsymbol{x})$, and the correlation of seismic performance is specified by the kernel function of $\varepsilon(\boldsymbol{x})$. For the intra-correlation of buildings that have exactly the same structural parameters, only a single GRF is required; for the inter-correlation between different types of buildings, a multiple-output GRF is needed and it is assumed to be a linear combination of a set of independent GRFs. Rational quadratic functions are selected as the form of kernel functions, and hyperparameters of kernel functions are determined by conducting Gaussian process regression using seismic performances observed during history scenario earthquakes.

The proposed method is applied to a portfolio of buildings in which there are 4 different types of buildings, and the following conclusions can be drawn.

- The results from the example closely-distributed portfolio of buildings indicate that seismic performances cannot be assumed perfect correlation, even when these buildings have exactly the same structural parameters and the spatial distance between adjacent buildings is as small as 20 m. Because the intra-correlation of buildings may have a high decay rate. By contrast, assuming independence is a better choice.
- Both the case studies of closely-distributed and sparsely-distributed buildings demonstrate that using the proposed GRF-based model to consider correlation can lead to a higher probability of occurrence of extreme seismic losses.
- As for magnitude-based regional loss assessment, the effects of spatial correlation of seismic performances can be overlooked as long as the uncertainties and correlations of IM fields have been considered.

However, some technical details about this method should be further investigated in future research. (1) How many and what history scenario earthquakes and ground motion records should be used to come to a balance between accuracy and efficiency of determining hyperparameters and to properly represent the decay rate of spatial

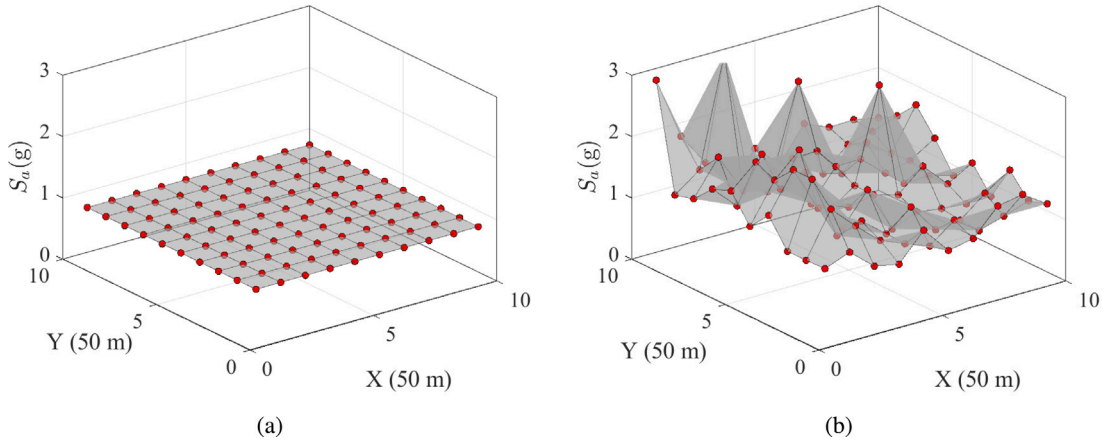

Fig. 12. (a) Median intensity S_a (T = 1.1 s) and (b) simulated random intensity field S_a (T = 1.1 s) of a scenario earthquake with M_w = 8.

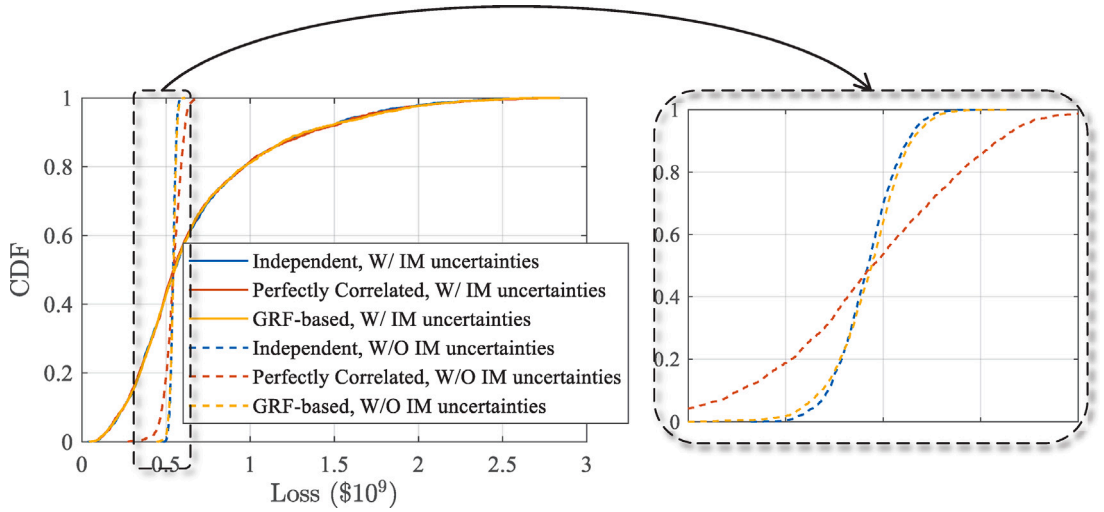

Fig. 13. CDFs of regional repair cost conditioned on M_w = 8.

correlation. (2) The algorithm of searching for the optimal hyperparameters can be improved to be more robust and rapid. (3) If the consequences of history scenario earthquakes are not serious enough, only a small fraction of buildings would collapse, which makes it difficult to determine the spatial correlation of collapse capacity of buildings. (4) Only the similarities of architectural and structural designs (e.g. number of stories and structural types) are considered in the proposed model, while the uncertainties and correlations of structural parameters (e.g. material strength, beam and column sizes), which may be caused by the building contractors, are not taken into account.

CRediT authorship contribution statement

Tian You: Conceptualization, Methodology, Data curation, Software, Formal analysis, Visualization, Validation, Investigation, Writing – original draft. **Wei Wang:** Supervision, Project administration, Funding acquisition. **Yiyi Chen:** Supervision, Project administration, Funding acquisition. **Solomon Tesfamariam:** Writing – review & editing.

Declaration of competing interest

The authors declare that they have no known competing financial interests or personal relationships that could have appeared to influence the work reported in this paper.

Data availability

Data will be made available on request.

Acknowledgment

The financial supports from the Natural Science Foundation of China (NSFC) under Grant Nos. 51820105013 and the Top Discipline Plan of Shanghai Universities-Class I with Grant No. 2022-3-YB-18 are gratefully acknowledged.

References

[1] Du A, Padgett JE, Shafieezadeh A. Influence of intensity measure selection on simulation-based regional seismic risk assessment. Earthq Spectra 2020;36(2):647–72. http://dx.doi.org/10.1177/8755293019891717.

[2] Goda K, Hong HP. Estimation of seismic loss for spatially distributed buildings. Earthq Spectra 2008;24(4):889–910. http://dx.doi.org/10.1193/1.2983654.

[3] Miano A, Jalayer F, De Risi R, Prota A, Manfredi G. Model updating and seismic loss assessment for a portfolio of bridges. Bull Earthq Eng 2016;14(3):699–719. http://dx.doi.org/10.1007/s10518-015-9850-y.

[4] Sabetta F, Pugliese A. Estimation of response spectra and simulation of nonstationary earthquake ground motions. Bull Seismol Soc Am 1996;86(2):337–52. http://dx.doi.org/10.1785/bssa0860020337.

[5] Rezaeian S, Der Kiureghian A. Simulation of synthetic ground motions for specified earthquake and site characteristics. Earthq Eng Struct Dyn 2010;39(10):1155–80. http://dx.doi.org/10.1002/eqe.997.

[6] Rodgers AJ, Pitarka A, Petersson NA, Sjögreen B, McCallen DB. Broadband (0–4 Hz) ground motions for a magnitude 7.0 Hayward fault earthquake with three-dimensional structure and topography. Geophys Res Lett 2018;45(2):739–47. http://dx.doi.org/10.1002/2017GL076505.
[7] Xiong C, Lu XZ, Guan H, Xu Z. A nonlinear computational model for regional seismic simulation of tall buildings. Bull Earthq Eng 2016;14(4):1047–69. http://dx.doi.org/10.1007/s10518-016-9880-0.
[8] Baker JW, Jayaram N. Correlation of spectral acceleration values from NGA ground motion models. Earthq Spectra 2008;24(1):299–317. http://dx.doi.org/10.1193/1.2857544.
[9] Goda K, Hong HP. Spatial correlation of peak ground motions and response spectra. Bull Seismol Soc Am 2008;98(1):354–65. http://dx.doi.org/10.1785/0120070078.
[10] Goda K, Atkinson GM. Intraevent spatial correlation of ground-motion parameters using SK-net data. Bull Seismol Soc Am 2010;100(6):3055–67. http://dx.doi.org/10.1785/0120100031.
[11] Loth C, Baker JW. A spatial cross-correlation model of spectral accelerations at multiple periods. Earthq Eng Struct Dyn 2013;42(3):397–417. http://dx.doi.org/10.1002/eqe.2212.
[12] Markhvida M, Ceferino L, Baker JW. Modeling spatially correlated spectral accelerations at multiple periods using principal component analysis and geostatistics. Earthq Eng Struct Dyn 2018;47(5):1107–23. http://dx.doi.org/10.1002/eqe.3007.
[13] Heresi P, Miranda E. Uncertainty in intraevent spatial correlation of elastic pseudo-acceleration spectral ordinates. Bull Earthq Eng 2019;17(3):1099–115. http://dx.doi.org/10.1007/s10518-018-0506-6.
[14] Eads L, Miranda E, Lignos DG. Average spectral acceleration as an intensity measure for collapse risk assessment. Earthq Eng Struct Dyn 2015;44(12):2057–73. http://dx.doi.org/10.1002/eqe.2575.
[15] O'Reilly GJ. Limitations of Sa(T1) as an intensity measure when assessing non-ductile infilled RC frame structures. Bull Earthq Eng 2021;19(6):2389–417. http://dx.doi.org/10.1007/s10518-021-01071-7.
[16] Gunay S, Mosalam KM. PEER performance-based earthquake engineering methodology, revisited. J Earthq Eng 2013;17(6):829–58. http://dx.doi.org/10.1080/13632469.2013.787377.
[17] Vamvatsikos D, Cornell CA. Incremental dynamic analysis. Earthq Eng Struct Dyn 2002;31(3):491–514. http://dx.doi.org/10.1002/eqe.141.
[18] FEMA. Seismic performance assessment of buildings (FEMA P-58). Report, FEMA; 2012.
[19] Budnitz RJ. Correlation of seismic performance in similar SSCs (structures, systems, and components). United States Nuclear Regulatory Commission; 2017.
[20] Reed J, Mc Cann Jr. M, Iihara J, Tamjed H. Analytical techniques for performing probabilistic seismic risk assessment of nuclear power plants. In: Structural safety and reliability. 1985.
[21] Segarra JD, Bensi M, Modarres M. A Bayesian network approach for modeling dependent seismic failures in a nuclear power plant probabilistic risk assessment. Reliab Eng Syst Saf 2021;107678.
[22] Zhou TT, Modarres M, Droguett EL. An improved multi-unit nuclear plant seismic probabilistic risk assessment approach. Reliab Eng Syst Saf 2018;171:34–47. http://dx.doi.org/10.1016/j.ress.2017.11.015.
[23] Erdik M, Sesetyan K, Demircioglu MB, Hancilar U, Zulfikar C. Rapid earthquake loss assessment after damaging earthquakes. Soil Dyn Earthq Eng 2011;31(2):247–66. http://dx.doi.org/10.1016/j.soildyn.2010.03.009.
[24] Silva V. Uncertainty and correlation in seismic vulnerability functions of building classes. Earthq Spectra 2019;35(4):1515–39. http://dx.doi.org/10.1193/013018eqs031m.
[25] DeBock DJ, Garrison JW, Kim KY, Liel AB. Incorporation of spatial correlations between building response parameters in regional seismic loss assessment. Bull Seismol Soc Am 2014;104(1):214–28. http://dx.doi.org/10.1785/0120130137.
[26] DeBock DJ, Liel AB. A comparative evaluation of probabilistic regional seismic loss assessment methods using scenario case studies. J Earthq Eng 2015;19(6):905–37. http://dx.doi.org/10.1080/13632469.2015.1015754.
[27] Heresi P, Miranda E. Structure-to-structure damage correlation for scenario-based regional seismic risk assessment. Struct Saf 2022;95:102155. http://dx.doi.org/10.1016/j.strusafe.2021.102155.
[28] Williams CK, Rasmussen CE. Gaussian processes for machine learning, vol. 2. MA: MIT press Cambridge; 2006.
[29] Duvenaud D. Automatic model construction with Gaussian processes. (Ph.D. thesis), 2014, http://dx.doi.org/10.17863/CAM.14087.
[30] Campbell KW, Bozorgnia Y. NGA-West2 ground motion model for the average horizontal components of PGA, PGV, and 5% damped linear acceleration response spectra. Earthq Spectra 2014;30(3):1087–115. http://dx.doi.org/10.1193/062913eqs175m.
[31] Dávalos H, Miranda E. A ground motion prediction model for average spectral acceleration. J Earthq Eng 2021;25(2):319–42. http://dx.doi.org/10.1080/13632469.2018.1518278.
[32] Jayaram N, Baker JW. Correlation model for spatially distributed ground-motion intensities. Earthq Eng Struct Dyn 2009;38(15):1687–708. http://dx.doi.org/10.1002/eqe.922.
[33] Teh YW, Seeger M, Jordan MI. Semiparametric latent factor models. In: International workshop on artificial intelligence and statistics. PMLR; 2005, p. 333–40.
[34] Fang C, Zhong Q, Wang W, Hu S, Qiu C. Peak and residual responses of steel moment-resisting and braced frames under pulse-like near-fault earthquakes. Eng Struct 2018;177:579–97.
[35] McKenna F. OpenSees: a framework for earthquake engineering simulation. Comput Sci Eng 2011;13(4):58–66. http://dx.doi.org/10.1109/MCSE.2011.66.
[36] FEMA. Quantification of building seismic performance factors (FEMA P695). Report, U.S. Dept. of Homeland Security, FEMA; 2009.
[37] Ancheta TD, Darragh RB, Stewart JP, Seyhan E, Silva WJ, Chiou BS-J, et al. NGA-West2 database. Earthq Spectra 2014;30(3):989–1005.
[38] Sun H, Burton H, Zhang Y, Wallace J. Interbuilding interpolation of peak seismic response using spatially correlated demand parameters. Earthq Eng Struct Dyn 2018;47(5):1148–68. http://dx.doi.org/10.1002/eqe.3010.
[39] Boore DM, Gibbs JF, Joyner WB, Tinsley JC, Ponti DJ. Estimated ground motion from the 1994 Northridge, California, earthquake at the site of the interstate 10 and La Cienega Boulevard bridge collapse, West Los Angeles, California. Bull Seismol Soc Am 2003;93(6):2737–51. http://dx.doi.org/10.1785/0120020197.